Chapter 1

LATERAL INHIBITION AND SPECTRAL OPPONENCY IN THE OUTER RETINA OF PRIMATE

1.1 Abstract

Horizontal cells in vertebrate retina provide the first layer of lateral inhibition in the visual stream. They have been hypothesized to play important roles in gain scaling photoreceptor signals to control for fluctuations in brightness and are assumed to play a role in color processing. We describe here a model of the outer retina that includes a trichromatic cone mosaic and two types of horizontal cell populations. Parameters of the horizontal cell network that influence the spatial sampling and chromatic opponency of first-order projection neurons, bipolar cells, were examined. The results point to substantial differences in the parameters necessary to produce dynamics mimicking those observed experimentally in two subpopulations of horizontal cells. Our analysis further highlights the potential impact of a previously overlooked retinal pathway for S-cone signals on color vision and offers insights into the visual functioning of individuals with congenital stationary night-blindness.

1.2 Introduction

A central goal of neuroscience is to understand how neuronal circuits give rise to human perception. Studying the contribution of inhibitory inter-neurons to information processing has been particularly limited by the tools available for modulating the activity of a single class of cells. The role of primate horizontal cells in visual processing provides one such example. Detailed anatomical descriptions have revealed the morphology and connections of this population of cells (Wässle et al., 1989; Ahnelt and Kolb, 1994a; Chan and Grünert, 1998). Single-cell electrophysiological measurements have provided a gross characterization

of their biophysical properties (Dacey et al., 1996; Lee et al., 1999; Smith et al., 2001; Dacheux and Raviola, 1990; Zhang et al., 2011; Lee et al., 2003). The footprint of horizontal cells on vision, however, has been more difficult to tease apart. We have approached this problem by developing a population model of outer retinal physiology.

Lateral inhibition introduced by horizontal cells produces spatial antagonism between a cone and its neighbors. The functional impact of this lateral inhibition on vision has been considered from at least three perspectives. One has focused on the potential importance of surround inhibition on sharpening edges and enhancing contrast of the visual image. By introducing a comparison of nearby cone activities, horizontal cells remove light patterns varying slowly in time or space, effectively acting to de-blur the image. Another perspective proposes that horizontal contribute to the computation of controlling for local and global fluctuations in brightness across a scene (Smith et al., 2001; Masland, 2011; Dacheux and Raviola, 1990). The third aspect of vision with which horizontal cells are often associated is color opponency.

Two types of horizontal cells, known as H1 and H2, are recognized in primates. The dendrites of H1 cells contact L- and M-cone terminals, but avoid S-cones, while the axonal arbor of H1 cells receives input from rods (Rodieck, 1998; Chan and Grünert, 1998; Dacey et al., 1996; Verweij et al., 1999; Ahnelt and Kolb, 1994b). H2 cells have dendrites that collect input from all three cones types and have an axon with processes that also receives input from cones (Rodieck, 1998; Ahnelt and Kolb, 1994b). Both types of primate horizontal cells hyperpolarize in response to all wavelengths of visible light (Dacey et al., 1996; Lee et al., 1999; Smith et al., 2001; Dacheux and Raviola, 1990; Zhang et al., 2011; Dacey et al., 2000b). Partly due to the lack of spectral opponency, early work argued that primate horizontal cells exclusively participate in achromatic vision (Dacheux and Raviola, 1990). In comparison, fish horizontal cells exhibit spectral opponency; they hyperpolarize to some wavelengths and depolarize to others (Daw, 1967; Svaetichin and MaCnichol, 1959; Kamermans et al., 1998).

Despite a lack of spectral opponency, however, both H1 and H2 cells have more recently been implicated in the first stages of color processing (Dacey et al., 2000b, 1996; Lee et al.,

2010; Neitz and Neitz, 2011). H1 cells are likely to be involved in generating L-M opponency in midget bipolar cells through a random-wiring mechanism (Paulus and Kröger-Paulus, 1983; Crook et al., 2011). H1 cells may also mediate the aforementioned brightness regulation (Dacheux and Raviola, 1990; Smith et al., 2001; Lee et al., 2003, 1999) and could contribute to after-images and chromatic adaptation (van Hateren, 2007). H2 cells, on the other hand, may be involved in blue-yellow color vision (Schmidt et al., 2014; Kolb et al., 1997; Calkins, 2000), because they receive strong S-cone input (Dacey et al., 1996; Ahnelt and Kolb, 1994b). However, the exact role of H2 cells in blue-yellow circuitry has not been settled (Field et al., 2007; Crook et al., 2009). Field et al. (2007) have argued that the H2 contributes the major L+M inhibitory component to the small bistratified ganglion cells receptive field, which is widely thought to be the retinal basis of blue/yellow vision. On the other hand, Crook et al. (2009) contended that H2 cells serve only an indirect role in the small bistratified circuit.

The potential for H2 cells to shape the response of L- and M-cone circuits has received less attention. This is largely because they make far fewer connections with each L- and M-cone terminal (Dacey et al., 1996), which, together with the fact that H1 horizontal cells avoid contacts with S-cones, has focused attention on the role H2 cells play in S-cone processing. Yet, horizontal cell synapses are known to be reciprocal in all species studied (Thoreson and Mangel, 2012) and, therefore, a less often considered pathway is the impact of the H2 cells upon L- and M-cone circuits. Further motivating a consideration of this pathway is the recently discovered GABAergic feedforward pathway from H2 horizontal cells directly onto cone bipolar cells (Puller et al., 2014a). This pathway acts in concert with the feedback pathway and would enhance the encoding of surround signals when the cone terminal is already depolarized and indifferent to further surround driven depolarization (Puller et al., 2014a).

Finally, we were additionally motivated to study the propagation of S-cone signals in the outer retina by the recent discovery of individuals with mutations to the metabotropic glutamate receptor expressed in ON-bipolar cells, mGluR6. These people are clinically diagnosed as night blind because signals from rod terminals to ON-bipolar cells are interrupted

(Dryja et al., 2005) and rods do not contact an OFF-bipolar cell. Similarly, physiological evidence argues against the existence of an OFF-bipolar cell dedicated to S-cones (Evers and Gouras, 1986). Therefore, these individuals were also expected to exhibit S-cone mediated color deficits. However, color vision deficits of any kind are not associated with mutations to mGluR6 (Zeitz et al., 2015). These observation led us to consider the possibility that the H2 horizontal cells provide a small number of L- and M-cones with significant signal from nearby S-cones that could be utilized by the brain to preserve normal color vision in these individuals. Using known anatomical and physiological properties of primate horizontal cells we demonstrate the plausibility of this pathway and discuss the potential implications for normal color processing.

1.3 Methods

We modified a version of the working model (WM) framework that has been previously described (Baker and Bair, 2012). WM was developed as a model of feedforward projections in the visual stream. We focused on the retinal front end of WM and further specialized the network to model color processing in the outer retina. An advantage of studying and fine tuning this framework over other existing retinal models is that WM was designed to model cortical circuits. Therefore, the impact of parameters in the outer retina can be rapidly considered from the point of view of higher centers in the brain. For the current work, we focused on the impact of the outer retina on color processing early in the visual pathway.

Existing population models of retina do not explicitly model the cone mosaic, or horizontal cells at the detail necessary to probe specific questions about horizontal cell function (Martínez-Álvarez et al., 2013; Wohrer and Kornprobst, 2009; Pei and Qiao, 2010). Similarly, previously developed biophysical models of cones and horizontal cells, do not included a stimulus paradigm, bipolar cells or a trichromatic retina (van Hateren, 2005, 2007; Smith et al., 2008; Packer and Dacey, 2005). Lastly, an older linear model that used measured cone mosaics to estimate receptive fields of theoretical lateral geniculate nucleus (LGN) neurons was too general in its specification. This model did not explicitly consider horizontal cells

and neglected the time domain entirely (Lennie et al., 1991).

Model overview

A one-dimensional view of a signal passing through our model is shown in Fig. 1.1. A uniform white light pulse presented to the retina was filtered by the cone photoreceptors. The trichromatic cone mosaic transformed the white light stimulus (specified in RGB coordinates) into cone excitations at each time step. The activity of the cone mosaic was then propagated through two resistive meshes, which modeled the H1 and H2 horizontal cell networks. A difference between each cone and the sum of the two networks directly beneath the cone was computed to produce a bipolar cell layer.

Cones

The temporal filtering properties of cones were modeled as a biphasic low-pass filter (Schnapf et al., 1990, 1987; Smith et al., 2001). A low-pass filter was implemented as the difference between two Maxwell-Boltzmann distributions with a scaling constant controlling the relative height of each distribution:

$$response = M_{exc} - \alpha * M_{inh} \tag{1.1}$$

The width of each distribution, M_{exc} and M_{inh}, and the scaling constant, α, were specified to roughly reflect the kinetics described by Schnapf et al. (1990) and Schneeweis and Schnapf (1999). Recent recordings from macaque and other mammalian cone terminals by Cao et al. (2014) has convincingly demonstrated that photocurrent from cones are in fact not biphasic; directly confirming earlier studies of human electroretinogram (van Hateren and Lamb, 2006). However, inclusion of a biphasic filter does not affect the main result of our simulations and provides a convenient and efficient method for temporally filtering incoming visual stimuli in a reasonably realistic manner.

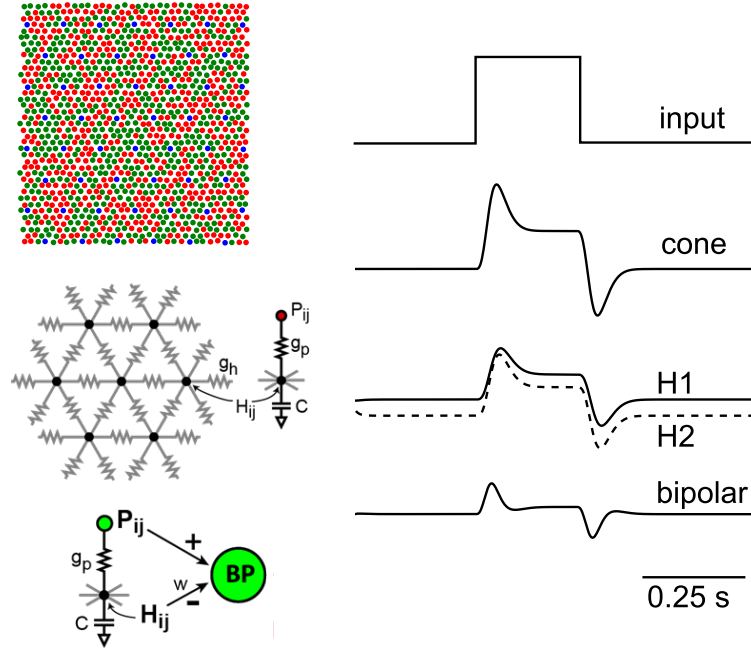Each cone in the mosaic of about 6500 cones was designated as either an L-, M- or

Figure 1.1: Schematic of our model. On the left is a cartoon representation of each of the major components of the model. The right is an example of a full-field flash of light propagating through a single column in our model that consists of a cone, two horizontal cell networks and a bipolar cell that takes the difference of the cone activation from the two horizontal networks.

S-cone. In most simulations, the ratio of L- to M-cones was 1:1 and cone identities were randomly distributed. Analysis of mosaics from humans (Hofer et al., 2005a; Roorda et al., 2001) and non-human primates (Field et al., 2010; Mollon and Bowmaker, 1992) suggests the distribution of L/M-cones in the mosaic are roughly random, with a slight tendency for cone classes to clump. The overall percentage of S-cones in the mosaic was set to 4%, which is approximately the value reported in the literature for retinal locations on the foveal slope (Curcio et al., 1991; Hofer et al., 2005a). S-cones here were arranged in a perfectly crystalline mosaic. Outside of the central 1-2 degrees, where they are more disorderly, S-cones tend to be regularly spaced (Curcio et al., 1991). Finally, we also studied one mosaic of about 800 cones that had been previously classified with adaptive optics and densitometry (Sabesan et al., 2015). The L:M cone ratio of that mosaic was 1.9:1. In order to avoid edge effects during simulation, the mosaic was placed inside a larger mosaic with the same L:M ratio.

RGB stimuli – specified in space and time $(S(x, y, t))$ – were converted into cone activations following standard colorimetry procedures (Brainard and Stockman, 2010). For simplicity, and to achieve maximal cone isolating contrast, we assumed monochromatic RGB primaries of 625, 525 and 445 nm. An example of a system that could produce monochromatic lights with spatial control, as we assume here, was recently realized with a digital light processing projector system (Bayer et al., 2015). We used the 2 degree human cone fundamentals reported by Stockman and Sharpe (2000). RGB values were then transformed into L-, M-, S- values according to:

$$
\begin{bmatrix} L(\lambda) \\ M(\lambda) \\ S(\lambda) \end{bmatrix} = \begin{bmatrix} L_R & L_G & L_B \\ M_R & M_G & M_B \\ S_R & S_G & S_B \end{bmatrix} \begin{bmatrix} R(\lambda) \\ G(\lambda) \\ B(\lambda) \end{bmatrix} \tag{1.2}
$$

The 3x3 matrix $(L_R ...)$ represents the dot product of each RGB monochromatic primary with each LMS sensitivity function (Brainard and Stockman, 2010). The matrix obtained

from this process is specified below:

$$
\begin{bmatrix} L(\lambda) \\ M(\lambda) \\ S(\lambda) \end{bmatrix} = \begin{bmatrix} 0.436214 & 0.7625 & 0.057364 \\ 0.074228 & 0.914324 & 0.092431 \\ 0.0 & 0.016317 & 0.984351 \end{bmatrix} \begin{bmatrix} R(\lambda) \\ G(\lambda) \\ B(\lambda) \end{bmatrix} \tag{1.3}
$$

In situ, photoreceptors perform a roughly logarithmic transformation on the intensity of incoming light. Here a Frobenius norm was applied to the cone system matrix (Eq. 1.3) to produce relative cone activations; thereby discarding the absolute light levels of stimuli.

For analysis of cone specific signals, we constructed cone isolating stimuli by inverting the 3x3 matrix in Eq. 1.3 and multiplying the inverted matrix with the desired vector of L-, M-, S-cone activation values (Estevez and Spekreuse, 1982). All cone isolating stimuli were computed as a change in cone activation relative to a background condition where L-, M- and S-cone activity was equated.

Horizontal cells

Horizontal cells were modeled as a restive mesh (Naka and Rushton, 1967). The passive conductance of current through the mesh was implemented by solving the diffusion equation on a Cartesian resistive grid (or mesh). This grid has the same spatial dimensions as the stimulus, $S(x, y, t)$, but followed the hexagonal arrangement of the cone mosaic. For each grid point, the cone excitation of a single cone at the same x, y location was applied through a conductance, g_P. Connections to the six neighboring grid points influenced the node with a specified conductance, g_H. The ratio of g_P to g_H controls the space constant of the restive mesh. For example, for a one-dimensional chain, $L = \sqrt{g_h/g_p}$, where L is the characteristic length, i.e., the distance over which an input applied (and held constant) at one point decays to $1/e$ of its value.

Bipolar cells

Bipolar cells take the difference between the excitatory signal of cones and the inhibitory signal of horizontal cells:

$$bp(t) = cone(t) - (\beta * H1(t) + \gamma * H2(t)) \tag{1.4}$$

β and γ control the strength of the horizontal surround relative to the center. Each *bp* cell is centered on a single cone, and thus its location and excitatory drive is taken to be that of the cone. Recordings of primate bipolar cells indicate that the center and surround tend to be roughly balanced (Dacey et al., 2000a), which was approximated here. Asymmetries between the ON- and OFF-bipolar pathways were not modeled.

Parameters

We focused on three parameters of our model. 1) The conductance of photoreceptor signals into each horizontal mesh network, g_P. This parameter influences both the speed at which signals effect the horizontal networks and the spatial size of the horizontal cell receptive field. 2) The conductance between each node in the horizontal cell network, g_H, which also effects the lateral spread of signal through each horizontal cell network. 3) The weight, w, each type of horizontal cell contributed to the bipolar calculation (Eq. 1.4). The parameters assumed in our model are recorded in Table 1.1.

Table 1.1: Parameters of the model.

receptive field size	H1 g_P	H1 g_H	H1 w	H2 g_P	H2 g_H	H2 w
large	0.15	2.0	0.65	1.0	1.0	0.4
small	0.15	0.04	0.65	1.3	0.02	0.4

Analysis of model

The WM framework generates data in the ndata format (http://www.imodel.org/nd/). Responses to visual stimuli were all carried out in python (http://www.python.org) using the numpy (http://www.numpy.org/) and scipy libraries (http://www.scipy.org/).

Spatial frequency tuning curves were generated by varying the spatial frequency of achromatic drifting (8Hz) gratings at 50% contrast. The F1 response to each grating was averaged across five horizontal cells. The spatial receptive field was computed by measuring the spread of signal across each horizontal cell network in response to the activity of a single cone. Temporal constants were measured by artificially, instantaneously turning on all cones from an entirely dark stimulus to one that maximally drove all cones.

We were interested in the contribution of the outer retina to spectrally opponent neurons recorded later in the visual pathways. To facilitate a comparison with studies of LGN (Tailby et al., 2008b; Reid and Shapley, 2002; Derrington et al., 1984) and retinal ganglion cell neurons (Sun et al., 2006), we computed cone weights in our model midget bipolar cells. Midget bipolar cells project one-to-one to midget ganglion cells (Kolb and Marshak, 2003) in the central retina and make roughly one-to-one contacts with LGN neurons (Usrey et al., 1999; Cleland et al., 1971; Reid and Shapley, 1992). Cone weights were estimated with uniform, full-field cone-isolating stimuli following the procedure outlined by Reid and Shapley (2002). The bipolar response to each cone isolating stimulus was computed and the amplitude was normalized by the cone contrast achieved with each cone-isolating stimulus. Then the three weights were further normalized such that the weights of each cone summed to 1; i.e. $L_w + M_w + S_w = 1$. All cone weights were represented in plots following the convention of (Derrington et al., 1984). Since we did not create distinct models for ON and OFF bipolar cells, the signal from our single, ON-type, bipolar cell was inverted to create OFF-type responses for display in cone weight figures.

1.4 Results

Basic characterization of the model

The connectivity of H1 and H2 cells with each cone class was set to mimic those reported for primate (Dacey et al., 1996). We computed the response of both horizontal networks to a full-field, uniform stimulus designed to isolate the activity of individual cone populations. Cone isolating conditions were computed relative to a background set to produce equal activity across cone classes. As Fig. 1.2 displays, H1 cells had input from both L- and M-cones while H2 cells receives input from all three cone types with a strong contribution from S-cones. The weights of L- and M-cones into the H2 network were set to 1/10th of S-cones (Table 1.1). Despite this small contribution from each cone, L- and M-cones still contributed a significant proportion of the response because they constitute the majority of cones in the mosaic. The response to cone isolating stimuli of each horizontal network qualitatively reproduced reports from experimental recordings of these cells (Dacey et al., 1996).
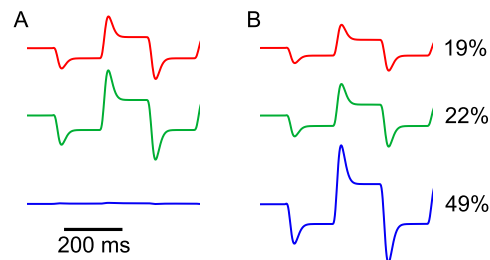

Figure 1.2: Response of modeled H1 and H2 cells to cone isolating stimuli. Increments and decrements of cone isolating stimuli relative to a background are shown for a modeled (**A**) H1 and (**B**) H2 cell. Red traces = L-cone isolating, green = M-cone isolating, blue = S-cone isolating. Cone contrast relative to the background is indicated to the right of the traces.

Fig. 1.3 displays the results of a basic linear systems characterization of the horizontal cells in our model. In Fig. 1.3A-C we adopted parameters that produced model cells closely mimicking the spatial receptive fields reported for H1 cells recorded from peripheral locations

(Packer and Dacey, 2002). In Fig. 1.3D-F we studied the impact of considerably smaller receptive fields on processing of visual signals in the outer retina. The parameters assumed in these two models are reported in Table 1.1. In both models, the conductance of H2 horizontal cells was adjusted such that the spatial spread of light evoked signal in this population was slightly smaller than H1 cells (Fig. 1.3A&D). This choice mirrored known differences in the spatial extent of horizontal cells: H2s receptive field are smaller than H1s, at least at peripheral eccentricities (Zhang et al., 2011). The temporal dynamics of H1 and H2 cells were adjusted to be approximately equal and with a time constant of 5-6 ms (Fig. 1.3B&E). This time constant was chosen to approximate the delay between center and surround measured in higher order neurons, which has been estimated to be on the order of 7-10 ms (Benardete and Kaplan, 1997; Reid and Shapley, 2002).

The response of horizontal cells to achromatic contrast of varying spatial frequency is shown in Fig. 1.3. Both networks displayed low pass characteristics. In the case of larger receptive fields, a sharp decline in response amplitude was observed beginning around 1 cycle/degree (Fig. 1.3). This relationship with spatial frequency closely agrees with experimental measurements of H1 cells at eccentric locations (Packer and Dacey, 2002). Intuitively, a low spatial frequency grating produces significant activation in all cones in the receptive field and thus elicits a strong hyperpolarization in the cell. Higher spatial frequencies drive only a subset of the cones in a given horizontal cell's receptive field and produce weaker a hyperpolarization. Following that logic, shrinking the size of the H2 receptive field still yields a low pass filter, but with a higher cut-off frequency. With fewer cones contributing to each horizontal cell receptive field, higher spatial frequencies that excite only a subset of the cones still produce strong hyperpolarizations because each cone provides a larger fraction of the overall drive into the horizontal cell (Fig.1.3).

Propagation of cone signals

We used cone isolating stimuli to explore the propagation of cone signals through the model networks.The signals in response to an S-cone isolating stimulus are shown for a single column
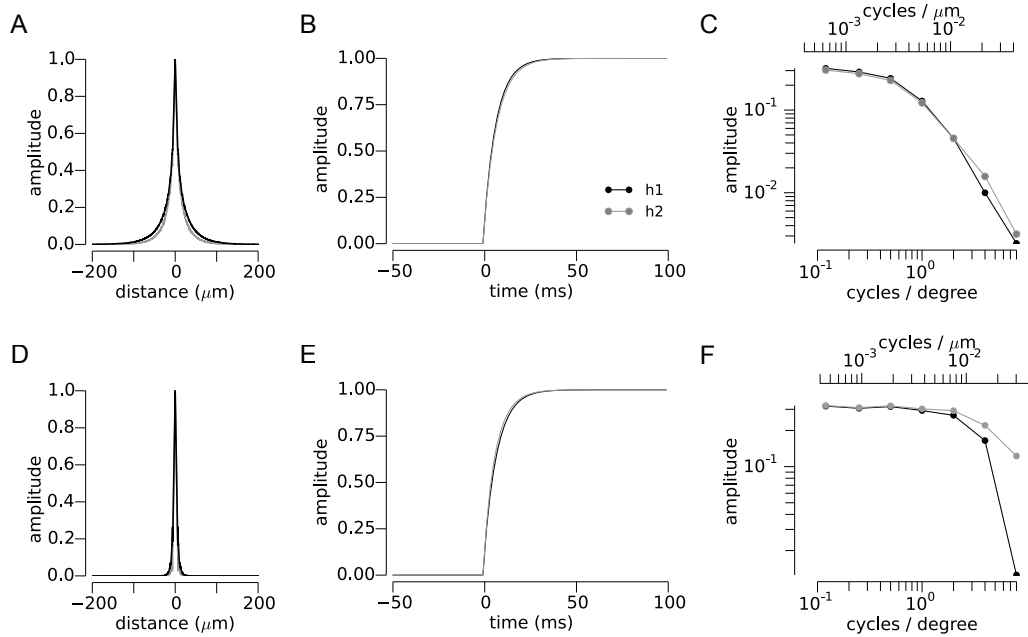
Figure 1.3: Spatial and temporal dynamics of horizontal cells. Two sets of parameters were studied for the H1 and H2 networks. **A-C** represent parameters that created behavior reflective of peripherally measured horizontal cell dynamics (Packer and Dacey, 2002). **D-F** are the results of the same analyses with parameters that produce a more spatially restricted receptive field.

of in our model in Fig. 1.4. Bipolar cells in our model take the difference between the visually driven excitation of a single M-cone, in this example, from H1 and H2 cells. As illustrated in Fig. 1.4, an S-cone isolating stimulus produces no visually evoked response in the M-cone or the H1 network. On the other hand, the H2 network was driven strongly by the stimulus because the M-cone was positioned directly adjacent to an S-cone. The weight each horizontal network contributes to this feedback operation has not been examined experimentally, so we varied the strength that the H2 network imposed on the M-cone center bipolar cell from 0.2 to 0.8. Not surprisingly, greater weights introduced a stronger S-cone signals into the bipolar cell. However, H2 cells make far fewer contacts with each L- and M-cone than S-cones, making large weights unlikely (Dacey, 1996). Therefore, we set the weight of the H2 network at a modest 0.4 in all simulations. The effect of changing this weight would be to scale all S-cone results in subsequent figures.

Impact of receptive field size

Technical constraints have confined experimental recordings from horizontal cells to peripheral locations. The most central eccentricity reported in the literature is about 4mm or 16-18 degrees from the fovea in the macaque (from an H1 cell). Over the peripheral areas tested, the size of H1 receptive fields scale with eccentricity (Packer and Dacey, 2002). However, whether this scaling continues to the central retina where dendritic field size of both H1 and H2 cells becomes very small is not known. It is possible that the dense gap junction coupling between cells could continue to produce effective receptive fields that extend far beyond the dendritic tree of any one horizontal cell.

The impact of receptive field size on cone weights to midget bipolar cells is explored in Fig. 1.5. We compared the signals in modeled bipolar cells under the assumption of both large and small horizontal cell receptive fields. When our model incorporated large receptive fields, cone weights did not vary substantially between bipolar cells because the surround of each bipolar pooled across many cones (Fig. 1.5A-B). In comparison, the more narrow receptive fields modeled in Fig. 1.5C-D produced substantially greater variability in
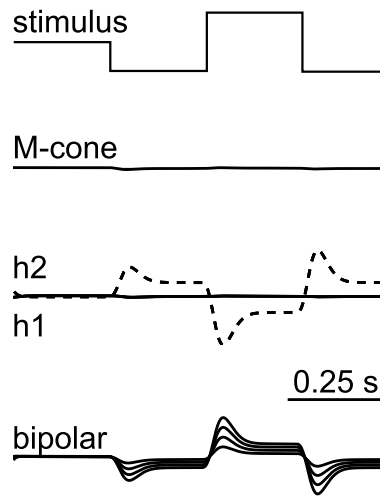
Figure 1.4: S-cone feedback onto a nearby M-cone. A single vertical column from the model is shown in response to an S-cone isolating stimulus. The M-cone and H1 cell (solid line) do not respond. The H2 cell (dotted line) is depolarized by the S-cone decrement and hyperpolarized by the S-cone increment. The impact of the horizontal cell signal is seen in the bipolar cell response, which reflects the difference between the M-cone and the H2 cell. The degree to which the H2 signal is reflected in the bipolar response is controlled by the parameter H2 w. Bipolar traces represent H2 w values ranging from 0.2 - 0.8 in increments of 0.2.

the weights of L/M-cones into the surround of bipolar cells. At central eccentricities, L- and M-cone weights into parvocellular neurons are more consistent with the variability we observed with small horizontal cell receptive fields (Derrington et al., 1984; Sun et al., 2006). This finding suggests that the receptive fields of foveal horizontal cells are in fact likely to be much smaller than those recorded in the periphery (Wässle et al., 1989, 2000).

Impact of network density

Anatomical descriptions of horizontal cells indicate that the density of connections in the networks of H1 and H2 cells may differ (Dacey et al., 1996; Wässle et al., 1989, 2000; Chan and Grünert, 1998). Both the number of cell bodies and the number of processes extended by H1 cells is higher than H2 cells. The consequence of a lower density of connections between H2 cells and the cone mosaic is that the electrical distance between any two cones will not always reflect their physical distance from one another. Because horizontal cells use passive conductance, two cones may occasionally be located next to each other but have less influence, via the H2 network, on one another than would be predicted by a denser network that supported the shortest path between each cone. We considered the potential impact of a lower density of processes in the H2 network by randomly eliminating connections between cones (i.e removing edges in Fig. 1.1).

Analysis of this less dense retinal network revealed fewer L/M-cone terminals receive S-cone input. Only a small smattering (11/100) of simulated cells, positioned close to an S-cones, received considerable input from S-cones (Fig. 1.6A). Importantly, roughly half the cells positioned close to an S-cone do not receive substantial S-cone input. This change in S-cone influence is also reflected in the cone weights (Fig. 1.6A). Compared to the previous example (Figure. 1.5), the majority of points fall on the edge of the diamond – indicating little influence from S-cones. Qualitatively, this plot resembles the population of LGN neurons reported by Tailby et al. (2008b) (their Fig 3B). Therefore, network density may be an important factor when considering the propagation of cone specific signals.
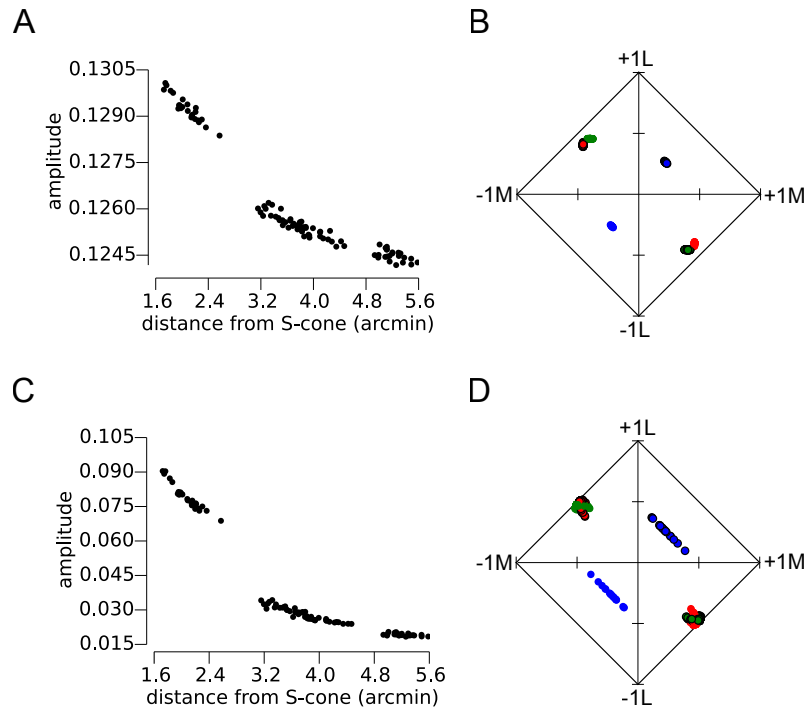
Figure 1.5: The dependence of cone weights on horizontal cell spatial receptive field. **A&B**. Horizontal cells with large spatial receptive fields are assumed. The amplitude of light evoked signal in response to an S-cone isolating stimulus was computed for 100 nodes in the H2 network and plotted as a function of that node from the nearest S-cone (**A**). There was substantial through out the H2 network with these parameters. **B**. Shows cone weights computed for bipolar cells in this model. Red dots represent L-cone centers, green=M-cone centers and blue dots indicate S-cone center bipolar cells. **C&D**. Same analysis but with much narrower spatial profile of horizontal cells. **C**. Significant S-cone signal is confined to H2 cells close to an S-cone. **D**. Same as **B** for the narrower horizontal cell receptive fields.
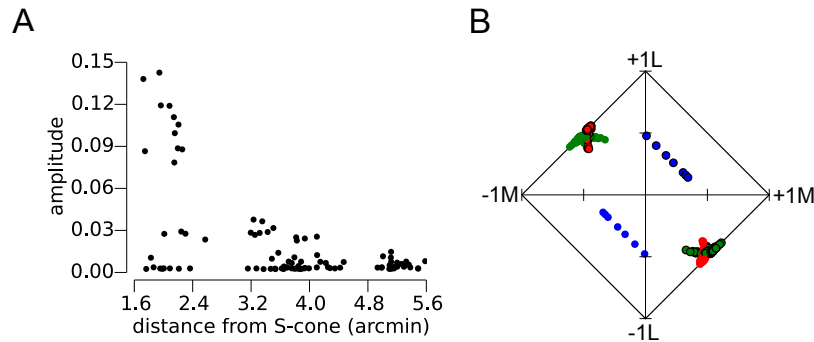
A

B

Figure 1.6: Cone inputs with a sparse H2 network. Same analysis as Fig. 1.5 for an H2 network with a lower density of connections between each node.

Impact of cone mosaic structure

L:M cone ratio is known to vary widely between individuals (Carroll et al., 2002; Hofer et al., 2005a). However, the impact of L:M cone ratio on color perception is subtle (Neitz et al., 2002; Schmidt et al., 2014). A previous modeling effort reported L:M ratio did not cause significant changes in LGN cone weights (Lennie et al., 1991). We changed the mosaic structure to study its potential impact on spectrally opponent cells. Changing the L:M cone ratio from 1:1 to 2:1 did not result in substantial changes in cone weights (Fig. 1.7A-C). The propagation of S-cone signals (Fig. 1.7B) was identical to Fig. 1.5C because the only difference between these two models are the L/M cone submosaics. Therefore, the impact of doubling the L:M cone ratio on the color information carried across the population of parvocellular neurons is subtle.

Near the fovea the spatial arrangement of S-cones becomes disorderly and indistinguishable from a random distribution (Curcio et al., 1991). We tested the potential influence of a random S-cone mosaic on outer retinal chromatic signaling. The results of this experiment are shown in Fig.1.7D-F. In a small number of cells (3/100), we observed large amplitude responses to S-cone isolating stimuli (Fig.1.7E). These cells resided near multiple S-cones. Due
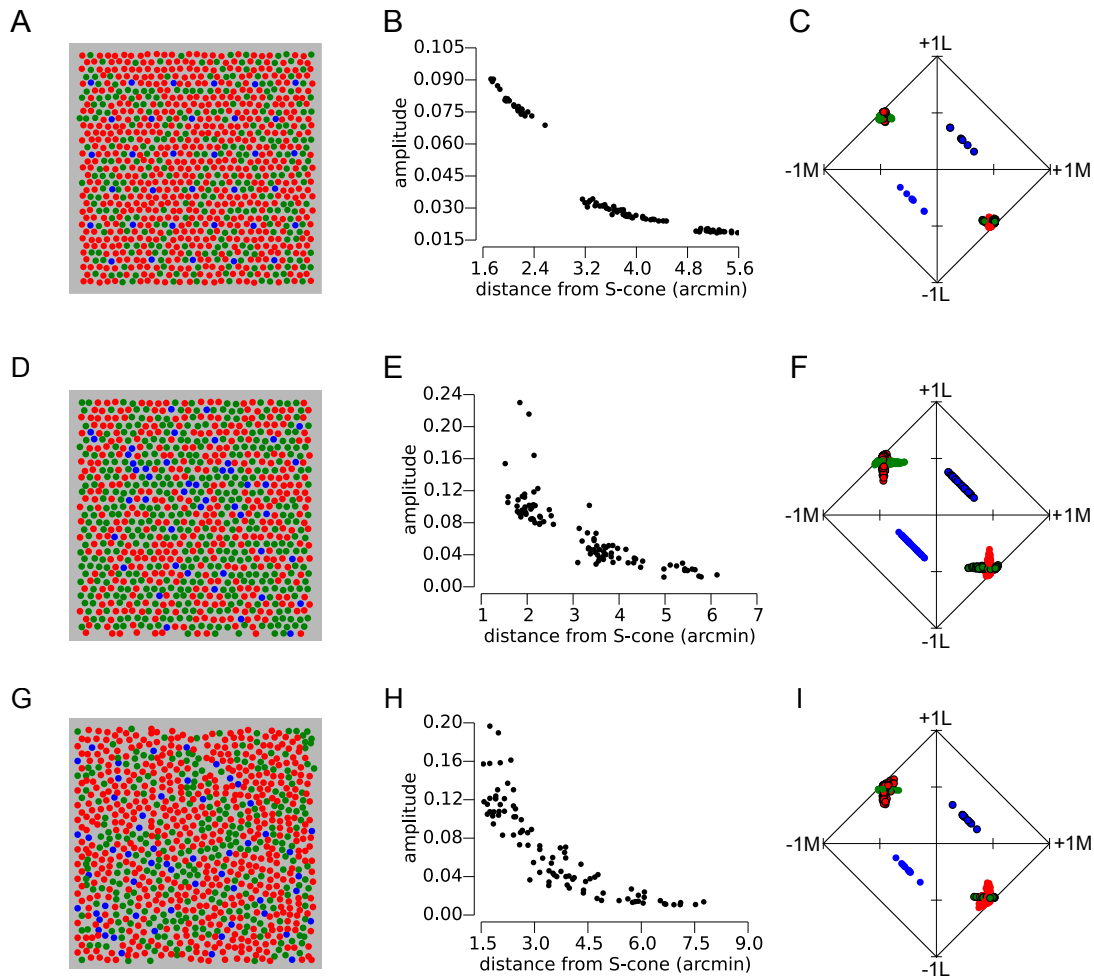
Figure 1.7: The influence of cone mosaic structure on cone weights. Cone weights were studied for three different mosaic structures. **A-C**. A mosaic with 4% S-cones and an L:M ratio of 2:1. **D-F**. A mosaic containing 4% S-cones that were randomly distributed and an L:M ratio of 1:1. **G-I**. A mosaic measured with adaptive optics and densitometry. Analyses otherwise were the same as Fig. 1.5.

to the increased scatter of S-cone amplitudes, cone weights were also more varied than the cone weights computed from otherwise identical parameters (compare Fig.1.5D to Fig.1.7E). In particular, a small number of L/M-cone center bipolar cells fell further from the edge of the diamond (Fig.1.7E) compared to the non-random S-mosaic (Fig.1.5D), indicating significant S-cone input.

The influence of the cone mosaic on color vision has drawn the attention of scientists for many decades (Williams et al., 1981b,a; Williams and Coletta, 1987; Williams et al., 1991; Roorda and Williams, 1999; Cicerone and Nerger, 1989; Carroll et al., 2002; Brainard et al., 2000; Neitz et al., 2002; Hofer et al., 2005b). The advent of adaptive optics microscopy (Williams, 2011) and the ability to image and stimulate single cones in the living human retina have brought the fine structure of the cone mosaic into consideration once again (Sincich et al., 2015). Our customizable model of the outer retina offers a simple and efficient manner for simulating responses in individual cone mosaics. The chromatic signature of modeled bipolar cells were computed for a measured cone mosaic (Fig.1.7G-I). This methodology could be useful in predicting the appearance of small spots delivered to classified retinas such as the one shown here.

Impact of spatial structure in the stimulus

Finally, we studied the interaction between the spatial content of the stimulus and the organization of the retinal mosaic. For this analysis we used the same mosaic structure and parameters as Fig. 1.7G-I. The influence of spatial structure on S-cone signals of theoretical bipolar cells is shown in Fig. 1.8. Compared to the same model measured with full-field, uniform lights (Fig. 1.7H), a 5 cycles/degree grating produced more restricted propagation of S-cone driven signals. These results suggest that spatial structure of light impinging upon the eye could have an important relationship with the manner in which cone specific signals routinely propagate through the horizontal cell network and influence downstream neurons. Importantly, natural scenes obey specific spatial characteristics (Dong and Atick, 1995; Atick and Redlich, 1992; Wachtler et al., 2001; Field, 1987). Therefore, the structure of light falling

on the retina should have important consequences for the algorithm used by the brain to classify cells as chromatic or achromtic (Wachtler et al., 2007; Brainard et al., 2008).
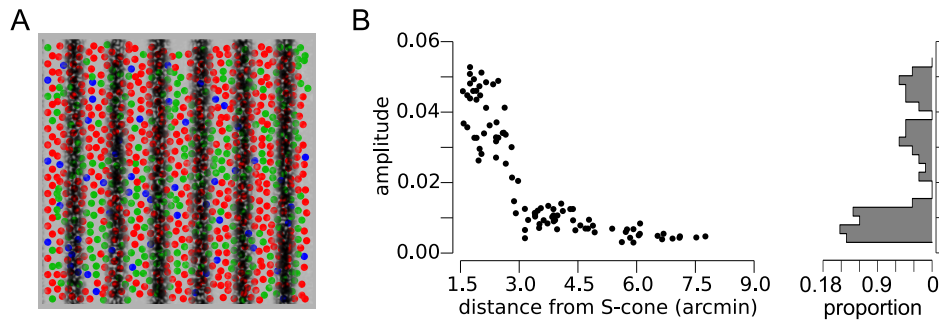

Figure 1.8: Spatial and temporal dependence of S-cone signal. An S-cone isolating grating of 5 cycles/degree was shown to the model mosaic in **A**. The amplitude of signals in H2 horizontal cells elicited by the S-isolating stimulus is recorded in **B**.

1.5 Discussion

We studied the influence horizontal cells impose on neural processing of light evoked signals in the context of color vision. Historically, unraveling the role of horizontal cells in vision has proven challenging because of the difficulty inherent in selectively modulating their activity in a behaving animal. Our motivation was to consider plausible horizontal cell networks and ask how the parameters of that model would influence color coding in the primate retina. Below we discuss our results in the context of what is know about horizontal cell physiology, the implications for color vision and the insight these studies offer for night blindness.

Horizontal cell physiology

As far as we are aware, our model represents the first time both H1 and H2 cell networks have been modeled simultaneously (Fig. 1.2). We found the connectivity patterns generated very different requirements for the conductances between cones and horizontal cells. Because H2 cells make fewer contacts with L- and M-cones which make up the bulk of cones in

primate mosaics, there is overall less excitatory drive into the horizontal cell network. To compensate for this loss of excitation, we had to increase the conductance of cones, g_P, into the H2 network relative to the H1 network by roughly a factor of 10 (Table 1.1). The ratio of this parameter to the horizontal cell conductance, g_H, controls the spatial constant, or receptive field size, of the horizontal cells. But g_P alone controls the time constant of the horizontal network. Without the large increase in g_P, the time constant of the H2 cells becomes unrealistically slow. Therefore, while we did not systematically study the parameter space of our models, the results point to an important difference between H1 and H2 cells: the signal between cones H2 cells is amplified relative to H1 cells. Uncovering the biological mechanism of this gain scaling should be an important goal for future experimental studies.

After settling on a set of parameters that reproduced the reported dynamics in the two horizontal cell networks we explored variations in known anatomical characteristics of these cells. The distribution and morphology of horizontal cells changes across the retina. The highest density of horizontal cells is in the central retina (Wässle et al., 1989; Chan and Grünert, 1998) where cone density is also highest (Curcio et al., 1990). The subtleties of this anatomical dependence on eccentricity also differs between H1 and H2 cells. Out to about 6 mm from the fovea, H1 cell are found at a higher density relative to H2 cells (Wässle et al., 1989). The size of each horizontal cell dendritic field also varies as a function of eccentricity (Packer and Dacey, 2002; Rodieck, 1998; Wässle et al., 1989). In the central retina, the dendritic trees of both H1 and H2 cells are small, contacting only a handful of nearby cones (Wässle et al., 1989). The size of the spatial receptive fields of H1 and H2 cells also differ (Zhang et al., 2011).

We modeled the impact of these changes with eccentricity. We found that narrow receptive fields were necessary to account for the distribution of cone responses that would be expected based on cone inputs measured in macaque retinal (Sun et al., 2006) and LGN neurons (Derrington et al., 1984; Reid and Shapley, 2002; Tailby et al., 2008b). Indeed, a prior study of cone inputs to LGN cells reported a similar relationship with cone weight distribution and the space constant of the surround (Lennie et al., 1991). This conclusion

is further supported by a quantitative analysis of L- and M-cone inputs to H1 cells. Dacey et al. (2000b) found large variability in the weights of each cone-type into the H1 cells that additionally varied predictably with eccentricity (Hagstrom et al., 2000). Together this evidence led to the hypothesis that H1 cells reflect the relative numerosity of cones in local regions of the retina. On the other hand if receptive fields were in fact large, the variability of cone weights into H1 cells should be very low in H1 cells from the same retinal region (Fig. 1.5A-B).

Horizontal cells are electrically coupled to cells of the same type through gap junctions (Zhang et al., 2011; Wässle et al., 2000; Chan and Grünert, 1998; Dacey et al., 1996). In fact, the degree to which they are coupled via gap junction has been suggested to underlie the difference in spatial receptive field size between H1 and H2 cells (Zhang et al., 2011). The potential role of gap junctions in primate outer retina on visual processing has been studied with models of cone mosaics (Hsu et al., 2000) and horizontal cells (Packer and Dacey, 2005). In the case of electrical coupling between primate horizontal cells, gap junctions are thought to introduce a second component – with a conductance distinct from the cable properties of the cells dendrites – to the receptive field that extends its spatial extent. Packer and Dacey (2005) further argued this extension added by gap junctions produced the irregularities in spatial tuning curves that they observed in some cells. Here, we assumed a simplified continuous resistive sheet producing only a single exponentially decaying spatial receptive field (Naka and Rushton, 1967). We found that peculiarities of spacing in the cone mosaic could also contribute to irregularities observed in measured spatial frequency tuning curve (Packer and Dacey, 2005). A pure exponential receptive field would produce a perfectly smooth tuning curve. However, even in the averages shown from our models in Fig. 1.3 a hint of irregularity can be seen that is attributable to the variability in distances between neighboring cones.

The mechanism and site of horizontal cell feedback has been a source of some controversy (Hirasawa et al., 2012). Recordings from L-, M-, and S-cone terminals in monkey have revealed at least some surround antagonism is present in the cones themselves (Packer et al.,

2010; Verweij et al., 2003). A second site of horizontal cell action that has persisted in the literature for many decades, but has yet to be demonstrated definitively, is a feed-forward pathway directly onto the dendritic tips of bipolar cells (Thoreson and Mangel, 2012). Historically, the evidence for this pathway has largely come from non-primate species and the existence of such a pathway in primates has been considered dubious. However, recently, the machinery necessary to support a feed-forward pathway from H2 onto cone-bipolar cells was reported in humans and non-human primates (Puller et al., 2014a,b).

In the current model, we simplified the cone-horizontal cell synapse by keeping the activity of each separate. The influence of horizontal cells was introduced only in the bipolar cells, which took the difference of these signals. Future iterations of the model will explicitly model the feedback and potential feedforward pathways of the horizontal cell network. The addition of a feedfoward pathway would serve to strengthen the surround inhibition of H2 cells and potentially add important temporal and spatial interactions between cones, bipolar cells and horizontal cells. It has been suggested that strong H1 feedback onto cone pedicles together with H2 feedforward signals into bipolar dendrites could create double opponency in the outer retina (Schmidt et al., 2014).

Kolb et al. (1997) has suggested that H2 cells do not reciprocate their signal onto L- and M-cones. The authors reason that if H2 do cells feedback, L/M-cone terminals should display S-cone opponency. Since H1 cells draw from L/M-cone terminals, an S-cone opponent signal should further be reflected in the signals of H1 cells. The consistent lack of S-opponent signal in H1 cells (Dacey et al., 1996, 2000b), they argue, offers indirect evidence that H2 cells do not feedback onto L- and M-cone terminals. Our results present one reason why H1 cells do not routinely exhibit S-opponency: S-cone driven signals in H2 cells does not propagate throughout the entire network. Only a minority of L/M-cones receive substantial S-cone input. Therefore, any S-opponent signal that might be recorded in H1 horizontal cells is swamped by the majority of L/M-cone input that does not receive S-cone signal. Further, the site of strongest H2 input to L- and M-center midget pathways may be the feedforward mechanism described above.

Implications for night blindness

The current work focused on the propagation of S-cone signals in the outer retina. The neural circuitry that carries S-cone driven signals to the brain is distinct from that of the L- and M-cones (Calkins, 2001; Miyagishima et al., 2014). S-cone terminals are contacted by a bipolar cell that makes specific contacts with 2-3 S-cones in the fovea and avoid L- or M-cone terminals (Mariani, 1984). The S-cone bipolar cell then in turn makes robust excitatory contacts with the small bistratified ganglion cell (Calkins et al., 1998; Crook et al., 2009; Dacey and Lee, 1994), which is widely believed to serve as the retinal output of S-cone driven signals (Solomon and Lennie, 2007; Lee et al., 2010). The S-cone bipolar cell, like other ON-type bipolar cells, uses the metabotropic glutamate receptor, mGluR6, to invert the signal from hyperpolarized cone terminals – thus encoding an excitatory, ON-response, to decreased glutamate release. Application of the mGluR6 agonist L-AP4, completely abolishes the S-cone signal in small bistratified cells measured with whole cell electrophysiology (Crook et al., 2009). Since no other S-cone specific pathway has been firmly established in primate (Miyagishima et al., 2014), the absence of a functioning mGluR6 protein should produce profound deficits in blue-yellow color vision, which is dependent upon S-cone signals.

A small group of individuals with mutations in the gene that codes for mGluR6, GRM6, have been identified. In response to light stimuli designed to isolate the ON pathway, electroretinograms confirm that signals from ON-bipolar cells are abolished (Dryja et al., 2005). Clinically, mutations to GRM6 that result in dysfunctional mGluR6 protein are associated with incomplete congenital stationary night blindness (Zeitz et al., 2015). This behavioral deficit arises because rod photoreceptors make exclusive contacts with a rod specific ON-type bipolar cell. In the absence of rod signal, these individuals are unable to see under low light, rod mediated conditions. With no established OFF-bipolar cell specific to S-cones, a similar deficit was expected in S-cone mediated color vision. However, paradoxically, the mutation in GRM6 does not produce measurable deficits in color vision. These subjects perform indistinguishably from controls on a wide range of color vision tests (Bijveld et al., 2013; Dryja

et al., 2005; Terasaki et al., 1999; Sergouniotis et al., 2012).

This finding suggests that S-cone signals are capable of exiting the retina through an alternative pathway that has yet to be characterized. Anatomical evidence has suggested an S-cone specific OFF bipolar cell may exist (Klug et al., 2003; Calkins, 2001), though these reports have been disputed (Neitz and Neitz, 2011) and physiological evidence is consistent with their absence (Evers and Gouras, 1986). Further, immunohistological double labeling of New World primate (marmoset) retina found OFF-midget bipolar cells avoided contact with S-cone terminals (Lee et al., 2005). Diffuse OFF-bipolar cells may make contacts with S-cones (Dacey et al., 2013). However, they indiscriminately sum input from L-, M- and S-cones. Therefore, they carry weak S-cone signals that are already mixed with L- and M-cone signals leaving them ill-suited to generate spectral opponency, even at higher centers in the brain.

Another potential route for S-cone signals to leave the retina, which we explored here, is through lateral inhibition via the H2 horizontal cell, which receives enhanced input from S-cones relative to L- and M-cones (Dacey, 1996). Here we provided a second plausible output for S-cone signals in individuals with deficits in ON-bipolar signaling. Our model highlights the plausibility that a small group of L- and M-cones residing nearby an S-cone would receive enough S-cone driven signal to produce the necessary spectral opponency in L- and M-center midget pathways to preserve normal color vision (Schmidt et al., 2014). The S-cone signal would contribute to the surround of both ON and OFF midget pathways thus creating four distinct forms of spectral opponency: L-(M+S) producing a yellow signal in an L-ON center, (M+S)-L producing a blue signal in an L-OFF, M-(L+S) producing a green signal in a M-ON and (L+S)-M producing a red signal in an M-OFF center. We further noted parameters of the outer retina that would influence the weights and relative numerosity of these S-opponent midget pathways.

Normal color processing

Lennie et al. (1991) concluded that S-cones made negligible contributions to the surrounds

of parvocellular neurons. Inclusion of S-cones to the surrounds produced cells that did not reflect the findings of (Derrington et al., 1984). More recent recordings from a larger number of macaque LGN neurons by the same group has uncovered a larger group of neurons with significant S-cone input (Tailby et al., 2008a). S-cones signals in peripheral midget ganglion cells have additionally been reported by (Field et al., 2010). The pathway through which S-cones traveled to generate the reported cone inputs is not know. S-cone signals in more central midget/parvocellular neurons have been carefully studied and are known to be rare (Sun et al., 2006; Derrington et al., 1984; Tailby et al., 2008b; Reid and Shapley, 2002). We report here the possibility of a pathway that would be expected to produce measurable, but modest S-cone input in a small minority (perhaps 2-10%) of midget bipolar cells. We estimate the weight of S-cone input would be in the range of 15-30%, which is all that is necessary to produce cells that would be well situated to code for hue percepts (Schmidt et al., 2014).

The idea that a majority of midget ganglion cells, with measurable L-M spectral opponency, contribute to a black/white pathway is on the surface untenable (De Valois and De Valois, 1993). The notion that all cells containing spectral opponency participate in color processing is inherent in almost every study of color processing. However, most parvocellular neurons often confuse red/green spots with black/white edges leaving them poorly suited to code for color vision (Wiesel and Hubel, 1966). We propose here that a combination of spatial structure in the input (Fig. 1.8), lower density of H2 network (Fig. 1.6) and irregularities of S-cone mosaic (Fig. 1.7D-I) could give rise to a small population of parvocellular neurons that would receive S-cone input and be ideally suited to signal color. The fact that parvocellular neurons provide robust projections to the ventral stream would allow higher cortical areas to categorize the output of these neurons as chromatic or achromatic based on experience. Learning which cells most reliably signal hue as opposed to those that confuse hue with black/white edges could be achieved with a cortical learning algorithm similar to the one proposed by Brainard et al. (2008). The majority of parvocellular neurons would provide a pathway for high resolution black and white, while activity of small few would

elicit red, green, blue or yellow (Schmidt et al., 2014).

REFERENCES

Ahnelt, P. and Kolb, H. (1994a). Horizontal cells and cone photoreceptors in human retina: a Golgi-electron microscopic study of spectral connectivity. *Journal of Comparative Neurology*, 343(3):406–27.

Ahnelt, P. and Kolb, H. (1994b). Horizontal cells and cone photoreceptors in primate retina: a Golgi-light microscopic study of spectral connectivity. *Journal of Comparative Neurology*, 343(3):387–405.

Atick, J. J. and Redlich, A. N. (1992). What does the retina know about natural scenes? *Neural Computation*, 210:196–210.

Baker, P. M. and Bair, W. (2012). Inter-Neuronal Correlation Distinguishes Mechanisms of Direction Selectivity in Cortical Circuit Models. *The Journal of Neuroscience*, 32(26):8800–8816.

Bayer, F. S., Paulun, V. C., Weiss, D., and Gegenfurtner, K. R. (2015). A tetrachromatic display for the spatiotemporal control of rod and cone stimulation. *Journal of Vision*, 15(11):1–16.

Benardete, E. A. and Kaplan, E. (1997). The receptive field of the primate P retinal ganglion cell, I: Linear dynamics. *Visual Neuroscience*, 14(1):169–85.

Bijveld, M. M. C., Florijn, R. J., Bergen, A. a. B., van den Born, L. I., Kamermans, M., Prick, L., Riemslag, F. C. C., van Schooneveld, M. J., Kappers, A. M. L., and van Genderen, M. M. (2013). Genotype and phenotype of 101 dutch patients with congenital stationary night blindness. *Ophthalmology*, 120(10):2072–81.

Brainard, D. H., Roorda, A., Yamauchi, Y., Calderone, J. B., Metha, A., Neitz, M., Neitz, J., Williams, D. R., and Jacobs, G. H. (2000). Functional consequences of the relative numbers of L and M cones. *Journal of the Optical Society of America. A*, 17(3):607–14.

Brainard, D. H. and Stockman, A. (2010). Colorimetry. In Bass, M., editor, *Vision and Vision Optics*, chapter 10, pages 1–56. McGraw-Hill, New York, 3 edition.

Brainard, D. H., Williams, D. R., and Hofer, H. (2008). Trichromatic reconstruction from the interleaved cone mosaic: Bayesian model and the color appearance of small spots. *Journal of Vision*, 8(5):1–23.

Calkins, D. J. (2000). Representation of cone signals in the primate retina. *Journal of the Optical Society of America A*, 17(3):597.

Calkins, D. J. (2001). Seeing with S cones. *Progress in retinal and eye research*, 20(3):255–87.

Calkins, D. J., Tsukamoto, Y., and Sterling, P. (1998). Microcircuitry and mosaic of a blue-yellow ganglion cell in the primate retina. *The Journal of Neuroscience*, 18(9):3373–85.

Cao, L.-H., Luo, D.-G., and Yau, K.-W. (2014). Light responses of primate and other mammalian cones. *Proceedings of the National Academy of Sciences of the United States of America*, 111(7):2752–7.

Carroll, J., Neitz, J., and Neitz, M. (2002). Estimates of L:M cone ratio from ERG flicker photometry and genetics. *Journal of Vision*, 2(8):531–542.

Chan, T. L. and Grünert, U. (1998). Horizontal cell connections with short wavelength-sensitive cones in the retina: a comparison between New World and Old World primates. *Journal of Comparative Neurology*, 393(2):196–209.

Cicerone, C. M. and Nerger, J. L. (1989). The relative numbers of long-wavelength-sensitive to middle-wavelength-sensitive cones in the human fovea centralis. *Vision Research*, 29(1):115–28.

Cleland, B. G., Dubin, M. W., and Levick, W. R. (1971). Simultaneous recording of input and output of lateral geniculate neurones. *Nature: New biology*, 231(23):191–192.

Crook, J. D., Davenport, C. M., Peterson, B. B., Packer, O. S., Detwiler, P. B., and Dacey, D. M. (2009). Parallel ON and OFF cone bipolar inputs establish spatially coextensive receptive field structure of blue-yellow ganglion cells in primate retina. *The Journal of Neuroscience*, 29(26):8372–87.

Crook, J. D., Manookin, M. B., Packer, O. S., and Dacey, D. M. (2011). Horizontal cell feedback without cone type-selective inhibition mediates "red-green" color opponency in midget ganglion cells of the primate retina. *The Journal of Neuroscience*, 31(5):1762–72.

Curcio, C. A., Allen, K. A., Sloan, K. R., Lerea, C. L., Hurley, J. B., Klock, I. B., and Milam, A. H. (1991). Distribution and morphology of human cone photoreceptors stained with anti-blue opsin. *Journal of Comparative Neurology*, 312:610–624.

Curcio, C. A., Sloan, K. R., Kalina, R. E., and Hendrickson, A. E. (1990). Human photoreceptor topography. *Journal of Comparative Neurology*, 292(4):497–523.

Dacey, D., Packer, O. S., Diller, L., Brainard, D., Peterson, B., and Lee, B. (2000a). Center surround receptive field structure of cone bipolar cells in primate retina. *Vision Research*, 40(14):1801–11.

Dacey, D. M. (1996). Circuitry for color coding in the primate retina. *Proceedings of the National Academy of Sciences of the United States of America*, 93:582–588.

Dacey, D. M., Crook, J. D., and Packer, O. S. (2013). Distinct synaptic mechanisms create parallel S-ON and S-OFF color opponent pathways in the primate retina. *Visual Neuroscience*, pages 1–13.

Dacey, D. M., Diller, L. C., Verweij, J., and Williams, D. R. (2000b). Physiology of L- and M-cone inputs to H1 horizontal cells in the primate retina. *Journal of the Optical Society of America. A*, 17(3):589–96.

Dacey, D. M. and Lee, B. B. (1994). The 'blue-on' opponent pathway in primate retina originates from a distinct bistratified ganglion cell type. *Nature*, 367:731–735.

Dacey, D. M., Lee, B. B., Stafford, D. K., Pokorny, J., and Smith, V. C. (1996). Horizontal cells of the primate retina: cone specificity without spectral opponency. *Science*, 271(5249):656–9.

Dacheux, R. F. and Raviola, E. (1990). Physiology of HI horizontal cells in the primate retina. *Proceedings of the Royal Society of London. Series B.*, 239(1295):213–230.

Daw, N. W. (1967). Goldfish Retina: Organization for Simultaneous Color Contrast Author. *Science*, 158(3803):942–944.

De Valois, R. L. and De Valois, K. K. (1993). A Multi-Stage Color Model. *Vision Research*, 33(8):1053–1065.

Derrington, A. M., Krauskopf, J., and Lennie, P. (1984). Chromatic mechanisms in lateral geniculate nucleus of macaque. *Journal of Physiology*, 357:241–65.

Dong, D. and Atick, J. (1995). Statistics of natural time-varying images. *Network: Computation in Neural Systems*, 6(3):345–358.

Dryja, T. P., Mcgee, T. L., Berson, E. L., Fishman, G. A., Sandberg, M. A., Alexander, K. R., Derlacki, D. J., and Rajagopalan, A. S. (2005). Night blindness and abnormal cone electroretinogram ON responses in patients with mutations in the GRM6 gene encoding mGluR6. *Proceedings of the National Academy of Sciences of the United States of America*, 102(12):4884–4889.

Estevez, O. and Spekreuse, H. (1982). The "silent substitution" method in visual research. *Vision Research*, 22:681–691.

Evers, H. U. and Gouras, P. (1986). Three cone mechanisms in the primate electroretinogram: two with, one without off-center bipolar responses. *Vision research*, 26(2):245–54.

Field, D. J. (1987). Relations between the statistics of natural images and the response properties of cortical cells. *Journal of the Optical Society of America. A*, 4(12):2379–94.

Field, G. D., Gauthier, J. L., Sher, A., Greschner, M., Machado, T. A., Jepson, L. H., Shlens, J., Gunning, D. E., Mathieson, K., Dabrowski, W., Paninski, L., Litke, A. M., and Chichilnisky, E. J. (2010). Functional connectivity in the retina at the resolution of photoreceptors. *Nature*, 467(7316):673–7.

Field, G. D., Sher, A., Gauthier, J. L., Greschner, M., Shlens, J., Litke, A. M., and Chichilnisky, E. J. (2007). Spatial properties and functional organization of small bistratified ganglion cells in primate retina. *The Journal of Neuroscience*, 27(48):13261–72.

Hagstrom, S. A., Neitz, M., and Neitz, J. (2000). Cone pigment gene expression in individual photoreceptors and the chromatic topography of the retina. *Journal of the Optical Society of America. A*, 17(3):527–37.

Hirasawa, H., Yamada, M., and Kaneko, A. (2012). Acidification of the synaptic cleft of cone photoreceptor terminal controls the amount of transmitter release, thereby forming the receptive field surround in the vertebrate retina. *The Journal of Physiological sciences*, 62(5):359–75.

Hofer, H., Carroll, J., Neitz, J., Neitz, M., and Williams, D. R. (2005a). Organization of the human trichromatic cone mosaic. *The Journal of Neuroscience*, 25(42):9669–79.

Hofer, H., Singer, B., and Williams, D. R. (2005b). Different sensations from cones with the same photopigment. *Journal of Vision*, 5:444–454.

Hsu, A., Smith, R. G., Buchsbaum, G., and Sterling, P. (2000). Cost of cone coupling to trichromacy in primate fovea. *Journal of the Optical Society of America A*, 17(3):635.

Kamermans, M., Kraaij, D. A., and Spekreijse, H. (1998). The cone/horizontal cell network: a possible site for color constancy. *Visual Neuroscience*, 15(5):787–97.

Klug, K., Herr, S., Ngo, I. T., Sterling, P., and Schein, S. (2003). Macaque retina contains an S-cone OFF midget pathway. *The Journal of Neuroscience*, 23(30):9881–7.

Kolb, H., Goede, P., Roberts, S., McDermott, R., and Gouras, P. (1997). Uniqueness of the S-cone pedicle in the human retina and consequences for color processing. *Journal of Comparative Neurology*, 386(3):443–60.

Kolb, H. and Marshak, D. (2003). The midget pathways of the primate retina. *Documenta Ophthalmologica*, 106:67–81.

Lee, B. B., Dacey, D. M., Smith, V. C., and Pokorny, J. (1999). Horizontal cells reveal cone type-specific adaptation in primate retina. *Proceedings of the National Academy of Sciences of the United States of America*, 96(25):14611–6.

Lee, B. B., Dacey, D. M., Smith, V. C., and Pokorny, J. (2003). Dynamics of sensitivity regulation in primate outer retina: the horizontal cell network. *Journal of Vision*, 3(7):513–26.

Lee, B. B., Martin, P. R., and Grünert, U. (2010). Retinal connectivity and primate vision. *Progress in Retinal and Eye Research*, 29(6):622–39.

Lee, S. C. S., Telkes, I., and Grünert, U. (2005). S-cones do not contribute to the OFF-midget pathway in the retina of the marmoset, Callithrix jacchus. *The European Journal of Neuroscience*, 22(2):437–47.

Lennie, P., Haake, P. W., and Williams, D. R. (1991). The Design of Chromatically Opponent Receptive Fields. In Landy, M. and Movshon, J. A., editors, *Computational Models of Visual Processing*, pages 71–82. The MIT Press.

Mariani, A. P. (1984). Bipolar cells in monkey retina selective for the cones likely to be blue-sensitive. *Nature*, 308:184–186.

Martínez-Álvarez, A., Olmedo-Payá, A., Cuenca-Asensi, S., Ferrández, J. M., and Fernández, E. (2013). RetinaStudio: A bioinspired framework to encode visual information. *Neurocomputing*, 114:45–53.

Masland, R. H. (2011). Cell populations of the retina: the Proctor lecture. *Investigative Ophthalmology & Visual Science*, 52(7):4581–91.

Miyagishima, K. J., Grünert, U., and Li, W. (2014). Processing of S-cone signals in the inner plexiform layer of the mammalian retina. *Visual Neuroscience*, 31(2):153–163.

Mollon, J. D. and Bowmaker, J. K. (1992). The spatial arrangement of cones in the primate fovea. *Nature*, 360:677–679.

Naka, K. I. and Rushton, W. A. H. (1967). The generation and spread of S-potentials in fish (Cyprinidae). *Journal of Physiology*, 192:437–461.

Neitz, J., Carroll, J., Yamauchi, Y., Neitz, M., and Williams, D. R. (2002). Color perception is mediated by a plastic neural mechanism that is adjustable in adults. *Neuron*, 35(4):783–92.

Neitz, J. and Neitz, M. (2011). The genetics of normal and defective color vision. *Vision Research*, 51(7):633–51.

Packer, O. S. and Dacey, D. M. (2002). Receptive field structure of H1 horizontal cells in macaque monkey retina. *Journal of Vision*, 2(4):272–92.

Packer, O. S. and Dacey, D. M. (2005). Synergistic center-surround receptive field model of monkey H1 horizontal cells. *Journal of Vision*, 5(11):1038–54.

Packer, O. S., Verweij, J., Li, P. H., Schnapf, J. L., and Dacey, D. M. (2010). Blue-yellow opponency in primate S cone photoreceptors. *The Journal of Neuroscience*, 30(2):568–72.

Paulus, W. and Kröger-Paulus, A. (1983). A new concept of retinal colour coding. *Vision Research*, 23(5):529–40.

Pei, Z. and Qiao, Q. (2010). An approximate retina model with cascade structures. *Proceedings - 2010 6th International Conference on Natural Computation, ICNC 2010*, 4(Icnc):2009–2012.

Puller, C., Haverkamp, S., Neitz, M., and Neitz, J. (2014a). Synaptic elements for GABAergic feed-forward signaling between HII horizontal cells and blue cone bipolar cells are enriched beneath primate S-cones. *PLoS ONE*, 9(2):e88963.

Puller, C., Manookin, M. B., Neitz, M., and Neitz, J. (2014b). A specialized synaptic pathway for chromatic signals beneath S-cone photoreceptors is common to human, Old and New World primates. *Journal of the Optical Society of America*, 31(4):A189–A194.

Reid, R. C. and Shapley, R. M. (1992). Spatial structure of cone inputs to the receptive fields in primate lateral geniculate nucleus. *Nature*, 356(6371):716–718.

Reid, R. C. and Shapley, R. M. (2002). Space and time maps of cone photoreceptor signals in macaque lateral geniculate nucleus. *The Journal of Neuroscience*, 22(14):6158–75.

Rodieck, R. W. (1998). *The First Steps in Seeing.* Sinauer Associates Inc, Sunderland, Massachusetts, 1 edition.

Roorda, A., Metha, A. B., Lennie, P., and Williams, D. R. (2001). Packing arrangement of the three cone classes in primate retina. *Vision Research*, 41(10-11):1291–306.

Roorda, A. and Williams, D. R. (1999). The arrangement of the three cone classes in the living human eye. *Nature*, 397(6719):520–2.

Sabesan, R., Schmidt, B. P., Tuten, W. S., and Roorda, A. (2015). Representation of color and achromatic percepts in the human cone mosaic. page in preparation.

Schmidt, B. P., Neitz, M., and Neitz, J. (2014). Neurobiological hypothesis of color appearance and hue perception. *Journal of the Optical Society of America A*, 31(4):A195–A207.

Schnapf, J. L., Kraft, T. W., and Baylor, D. A. (1987). Spectral sensitivity of human cone photoreceptors. *Nature*, 352:439–441.

Schnapf, J. L., Nunn, B. J., Meister, M., and Baylor, D. A. (1990). Visual transduction in cones of the monkey Macaca fasciularis. *Journal of Physiology*, 427:681–713.

Schneeweis, D. M. and Schnapf, J. L. (1999). The photovoltage of macaque cone photoreceptors: adaptation, noise, and kinetics. *The Journal of Neuroscience*, 19(4):1203–16.

Sergouniotis, P. I., Robson, A. G., Li, Z., Devery, S., Holder, G. E., Moore, A. T., and Webster, A. R. (2012). A phenotypic study of congenital stationary night blindness (CSNB) associated with mutations in the GRM6 gene. *Acta Ophthalmologica*, 90(3).

Sincich, L. C., Sabesan, R., Tuten, W. S., Roorda, A., and Harmening, W. M. (2015). Functional Imaging of Cone Photoreceptors. In Kremers, J., Baraas, R., and Marshal, J., editors, *Human Color Vision*, chapter 4. Springer, New York.

Smith, V. C., Pokorny, J., Lee, B. B., and Dacey, D. M. (2001). Primate Horizontal Cell Dynamics : An Analysis of Sensitivity Regulation in the Outer Retina. *Journal of Physiology*, 85:545–558.

Smith, V. C., Pokorny, J., Lee, B. B., and Dacey, D. M. (2008). Sequential processing in vision: The interaction of sensitivity regulation and temporal dynamics. *Vision Research*, 48(26):2649–56.

Solomon, S. G. and Lennie, P. (2007). The machinery of colour vision. *Nature Reviews. Neuroscience*, 8(4):276–86.

Stockman, A. and Sharpe, L. T. (2000). The spectral sensitivities of the middle- and long-wavelength-sensitive cones derived from measurements in observers of known genotype. *Vision Research*, 40(13):1711–37.

Sun, H., Smithson, H. E., Zaidi, Q., and Lee, B. B. (2006). Specificity of Cone Inputs to Macaque Retinal Ganglion Cells. *Journal of Neurophysiology*, 95:837–849.

Svaetichin, G. and MaCnichol, E. F. (1959). Retinal mechanisms for chromatic and achromatic vision. *Annals of the New York Academy of Sciences*, 74(2):385–404.

Tailby, C., Solomon, S. G., Dhruv, N. T., and Lennie, P. (2008a). Habituation reveals fundamental chromatic mechanisms in striate cortex of macaque. *The Journal of Neuroscience*, 28(5):1131–9.

Tailby, C., Solomon, S. G., and Lennie, P. (2008b). Functional asymmetries in visual pathways carrying S-cone signals in macaque. *The Journal of Neuroscience*, 28(15):4078–87.

Terasaki, H., Miyake, Y., Nomura, R., Horiguchi, M., Suzuki, S., and Kondo, M. (1999). Blue-on-Yellow Perimetry in the Complete Type of Congenital Stationary Night Blindness. *Investigative Ophthalmology & Visual Science*, 40(11):2761–2764.

Thoreson, W. B. and Mangel, S. C. (2012). Lateral interactions in the outer retina. *Progress in retinal and eye research*, 31(5):407–41.

Usrey, W. M., Reppas, J. B., and Reid, R. C. (1999). Specificity and strength of retinogeniculate connections. *Journal of neurophysiology*, 82(6):3527–3540.

van Hateren, J. H. (2005). A cellular and molecular model of response kinetics and adaptation in primate cones and horizontal cells. *Journal of Vision*, 5(4):331–347.

van Hateren, J. H. (2007). A model of spatiotemporal signal processing by primate cones and horizontal cells. *Journal of Vision*, 7(3):3.

van Hateren, J. H. and Lamb, T. D. (2006). The photocurrent response of human cones is fast and monophasic. *BMC Neuroscience*, 7(1):34.

Verweij, J., Dacey, D. M., Peterson, B. B., and Buck, S. L. (1999). Sensitivity and dynamics of rod signals in H1 horizontal cells of the macaque monkey retina. *Vision Research*, 39(22):3662–72.

Verweij, J., Hornstein, E. P., and Schnapf, J. L. (2003). Surround antagonism in macaque cone photoreceptors. *The Journal of Neuroscience*, 23(32):10249–57.

Wachtler, T., Doi, E., Lee, T.-w., and Sejnowski, T. J. (2007). Cone selectivity derived from the responses of the retinal cone mosaic to natural scenes. *Journal of Vision*, 7(8):1–14.

Wachtler, T., Lee, T.-W., and Sejnowski, T. J. (2001). Chromatic structure of natural scenes. *Journal of the Optical Society of America A*, 18(1):65–77.

Wässle, H., Boycott, B. B., and Rohrenbeck, J. (1989). Horizontal cells in the monkey retina: cone connections and dendritic network. *European Journal of Neuroscience*, 1:421–435.

Wässle, H., Dacey, D. M., Haun, T., Haverkamp, S., Grünert, U., and Boycott, B. B. (2000). The mosaic of horizontal cells in the macaque monkey retina: with a comment on biplexiform ganglion cells. *Visual Neuroscience*, 17(4):591–608.

Wiesel, T. N. and Hubel, D. H. (1966). Spatial and chromatic interactions in the lateral geniculate body of the rhesus monkey. *Journal of Neurophysiology*, 29(6):1115–56.

Williams, D. R. (2011). Imaging single cells in the living retina. *Vision Research*, 51(13):1379–96.

Williams, D. R. and Coletta, N. J. (1987). Cone spacing and the visual resolution limit. *Journal of the Optical Society of America. A*, 4(8):1514–23.

Williams, D. R., Macleod, D. A., and E, M. M. H. (1981a). Punctate sensitivity of the blue sensitive mechanism. *Vision Research*, 21:1357–1375.

Williams, D. R., Macleod, D. A., and Hayhoe, M. M. (1981b). Foveal tritanopia. *Vision Research*, 21:1241–1256.

Williams, D. R., Sekiguchi, N., Haake, W., Brainard, D., and Packer, O. (1991). The cost of trichromacy for spatial vision. In Valber, A. and Lee, B. B., editors, *From Pigments to Perception*, pages 11–21. Plenum Press, New York.

Wohrer, A. and Kornprobst, P. (2009). Virtual Retina: A biological retina model and simulator, with contrast gain control. *Journal of Computational Neuroscience*, 26(2):219–249.

Zeitz, C., Robson, A. G., and Audo, I. (2015). Congenital stationary night blindness: An analysis and update of genotypephenotype correlations and pathogenic mechanisms. *Progress in Retinal and Eye Research*, 45:58–110.

Zhang, A.-J., Jacoby, R., and Wu, S. M. (2011). Light- and dopamine-regulated receptive field plasticity in primate horizontal cells. *Journal of Comparative Neurology*, 519(11):2125–34.